Chemical stabilization of γ-polyglutamate by chitosan and the effect of co-solvents on the stability

Chemical stabilization of y-polyglutamate by chitosan and the effect of co-solvents on the stability

Marjan Motiei[a,b], Seyede Zohreh Mirahmadi-Zare[a,*], Mohammad Hossein Nasr-Esfahani[a]

[a]*Department of Animal Biotechnology, Cell Science Research Center, Royan Institute for Biotechnology, ACECR, 8159358686 Isfahan, Iran*

[b]*Centre of Polymer Systems, Tomas Bata University in Zlín, Třída Tomase Bati 5678, 76001 Zlín, Czech Republic*

[*]*Corresponding author at: Department of Animal Biotechnology, Cell Science Research Center, Royan Institute for Biotechnology, ACECR, 8159358686 Isfahan, Iran. E-mail address: mirahmadi_zare@royaninstitute.org (S.Z. Mirahmadi-Zare).*

ABSTRACT

In protein-based formulations, conformational distortions and attractive interactions may cause insoluble and undesired aggregates. In the case of ionic peptides, including cationic or anionic, commonly electrostatic interactions are the main factors that control structure assembling. In this study, it was proposed that grafting of chitosan (CS) to γ-polyglutamic acid (γPGA) might exhibit much strong inhibiting effect on the formation of protein aggregates due to multiple amino groups and hydrophilic properties. To guarantee stable and safe biopharmaceutical formulation, the potency of a variety of stabilizers including sugars (glucose, sucrose), polyols (sorbitol, glycerol), surfactant (Tween 20), salting-out salt (PBS), and also different pH values have been evaluated on stabilizing or destabilizing the native state of CS-g-PGA copolymer using FTIR, CD, DLS, and SDS-PAGE. The comparable analysis revealed that the stability of CS-g-PGA was strongly dependent on pH owing to the polyelectrolyte characteristics of the polymers. Altogether these results implied that CS at optimized conditions might be an important precursor for the pharmaceutical industry and function as a new polymer for aggregation suppression and protein stabilization.

Keywords: γ-polyglutamic acid, chitosan, chemical stabilization, protein folding, pH depending structure

1. Introduction

Aggregated proteins are one of the major side products of pharmaceutical processing and storage due to the dynamic and metastable structure of proteins. Thus, it is essential to stabilize the native conformational state of proteins against undesired and non-native aggregates [**1**]. Aggregation can be in the form of β-sheet fibrils or amorphous structures through a reversible or irreversible process that involves noncovalent (e.g., hydrogen bonding, hydrophobic, Van der Waals, and electrostatic interactions) and/or covalent interactions (e.g., disulfide and nondisulfide linkages) of several protein molecules [**2,3**]. The major reason underlying reversible aggregates is often considered to be caused by partially unfolding, misfolding, and self-assembly of protein molecules, which could be induced by changes in any of the quality control systems of protein (e.g., concentration, amino acid sequence, net charge) or external factors (e.g., temperature, pH, pressure, agitation, ionic strength, buffer species,

excipients, impurities, lyophilization, denaturing agents and hydrodynamic flow) [**4,5**]. In other words, any changes in physical properties of proteins such as hydrophobicity, sec-ondary/tertiary structure, and thermodynamic/kinetic barriers result in unfolding and increasing the aggregation [**6**]. For instance, higher aggregation is attributed to high temperatures, as Borzova et al. exhibited that the aggregation rate of bovine serum albumin increased with increasing the temperature (60 °C, 65 °C, 70 °C, and 80 °C) in phosphate buffer (0.1 M, pH 7.0) [**4**]. Nonetheless, Mehra et al. exhibited cryo-contraction of substrate-bound γ-*secretase* and its weakened β-sheet structure with temperature [**7**]. In another study, Dobsona et al. indicated that an extensional flow could unfold thermodynamically and kinetically stable proteins dependent on the protein sequence and structure [**5**]. However, there are some unique treatments, including the addition of polymers and co-solvents, and also changes in pH and ionic strength to manipulate protein-protein interactions in a suppressing or disrupting manner and probably capable of removing aggregates [**8,9**].

The polymers stabilize the proteins by protecting the exposed hydrophobic surfaces through electrostatic interactions or chemical modifications [**10**]. A variety of anionic and cationic polymers have been confirmed to be effective at stabilizing proteins and preventing aggregations [**11**]. Furthermore, CS as a cationic polymer with multiple amino groups and hydrophilic properties may be an ideal candidate in stabilizing an anionic polypeptide such as γ-PGA [**12,13**]. The use of poly-amino acids has been of tremendous interest in biomedical applications in recent years due to the possibility of being used as crosslinking agents and the ability to be functionalized through specific chemical groups [**1**]. γ-PGA is an anionic natural polypeptide composed of repetitive glutamic acid units (only D, only L, or both enantiomers), and the secondary structure in aqueous solution is described as a random coil and α-helix dependent on ionized and unionized form, respectively [**14,15**]. γ-PGA is a biodegradable, water-soluble, non-immunogenic and non-toxic biopolymer with antimicrobial activity [**16,17**]. This biopolymer with an isoelectric point of about 2.19 can be self-assembled or grafted with oppositely charged biopolymers such as CS with an isoelectric point of 6.5 to form polyelectrolyte complexes [**4**].

CS, a natural polymer of D-glucosamine and N-acetyl-D-glucosamine linked by β-(1,4)glycosidic bonds, might easily be prepared through partial or total deacetylation of chitin. This biopolymer is the most promising pharmaceutical and medical system due to unique properties such as biocompatibility, feasible biodegradability, low toxicity, low immunogenicity, antibacterial, and mechanically strong properties [**18**]. The combination of CS and γ-PGA by covalent or non-covalent linkage is a new emerging trend as building blocks of therapeutic vehicles. Further studies utilized non-covalent electrostatic interactions between γ-PGA and polymer chains [**19,20**], while the covalent binding between them is limited to polyethylene glycol [**21**] and poly(N-vinylpyrrolidone) [**22**]. In contrast to the non-covalent linkages that rely on the reversible electrostatic interaction between cationic and anionic units of polyelectrolyte complexes, an irreversible association can be followed by the formation of a covalent bond between electrophilic and nucleophilic centers in these polymers. This approach offers a variety of potential benefits and drawbacks, including high potency and prolonged duration of action against induction of aggregation and selfassociation reactions due to conformational distortion of protein [**23**]. In these cases, some structural parameters of polymer along with some buffer conditions play a major role in the chemical stability of polymer and co-polymer structures. For instance, related studies have shown that high concentrations of polymer and co-polymer chains lead to increasing nucleation and collisions with high probability, increasing in aggregate formation and particle diameter [**24,25**]. Kim et al. observed that an increase in nanostructure size was accompanied by an increase in Mw of CS [**26**]. Also, the degree of polymerization and the deacetylation ratio of CS on its repeating units influence its colloidal behavior and biological performance [**27**].

Among the buffer parameters, pH is the most common influencing factor that has been investigated to control the resulting structured parameters such as stability, size, charge, folding and so on. It can be discussed by the tendency of proteins to unfold partially at pH values far from isoelectric point [**9**] by increasing repulsive electrostatic forces, which play an important role in reducing the self-association of peptides. Therefore, pH, ionic strength, nature of ions, and the presence of polyelectrolytes affect the rate and extent of aggregation. A comprehensive and rigorous study has shown that the alkaline environments (pH 7.0-12.0), as opposed to acidic conditions (pH 2.0-6.0), keeps the secondary and tertiary structure of pyruvate dehydrogenase kinase-3 [**28**].

Furthermore, protein-stabilizing co-solvents including sugars, polyols, surfactants, and salting-out salts can provide the optimum conditions for maintaining γ-PGA stability. The impact of these co-solvents on protein stability is described to be dependent on the characteristics of co-solvents (type, concentration, and MW), proteins (type and concentration), and solvents (pH and ionic strength) [**1,9,11**]. Sugars and polyols are often used to stabilize proteins and protect them from aggregation. According to Prestrelski et al., disaccharides including sucrose, lactose, maltose, and trehalose are more effective stabilizers than monosaccharides, such as glucose and fructose [**29**]. They confirmed the infrared spectra of several proteins (e.g., bFGF, γ-IFN, α-lactalbumin, α-casein, and G-CSF) lyophilized with sucrose closely resemble the respective spectra of the same proteins in aqueous solution [**29**]. Among the polyols, sorbitol and glycerol have been shown to decrease the aggregation and increase the conformational stability of proteins by preferential hydration of the proteins [**11,30**]. However, Bauer et al. demonstrated that glycerol promoted the formation of aggregates for lysozyme at pH 3 and 9 as well as glucose oxidase at pH 9 due to its impact on dynamic viscosity [**9**]. A nonionic surfactant such as Tween 20 is another co-solvent that reduces protein aggregation, but impurities may result in oxidation reactions and subsequent conformational distortion, self-association, and aggregation of proteins. Therefore, the efficiency of these surfactants depends on the purity and also protein/ surfactant ratio [**23**].

The effect of salts on protein stability is also depending on the type (salting out and salting in) and concentration. According to Ohtake et al., salting-out salts can increase the stability of proteins, while the salting-in salts either decrease or demonstrate an insignificant effect on the stability of proteins [**11**]. In salting-out salts, the surface tension of the solution increases due to tight binding of ions to water and effective competing for hydration of the protein surface. In the presence of less water on the protein surface, the protein molecules self-associate and precipitate [**31**]. Kramer et al. exhibited that ammonium sulfate led to increasing of melting temperature of the proteins (e.g., human serum albumin and α-lactalbumin) by increasing the surface tension of bulk water, so the folded state was favored owing to reducing the water-protein interface in comparison with the unfolded state [**31**]. However, a low concentration of slating out salts was shown more conformational stability than a high concentration due to electrostatic shielding of attractive forces [**9**]. PBS as the most common biological buffer is a salting-out agent that supply desolvation and storage of proteins over a wide range of pH. So it can be used to study the effect of various pH values on the conformational stability of proteins due to the pH dependency of proteins.

While the synthesis of a wide range of copolymer structures is very difficult due to the comprehensive study of the effect of structural parameters of polymers including different charge and size and percentages of de-acetylation and grafting, but the effect of buffer conditions is easy to study. As a consequence, the main objective of this study is to explore the optimal conditions for preserving the native structure of y-PGA and inhibiting protein aggregation using CS-grafting. To this purpose, CS-g-PGA copolymer was synthesized and exposed unique compounds known to stabilize proteins such as co-solvents and salting-out agents within a wide range of pH. Then, the conformational properties

were evaluated using FTIR, CD, DLS, and SDS-PAGE techniques. Applying these techniques can aid in a greater fundamental understanding of the characteristics and roles of γ-PGA (or structurally similar polymers) that are found in the natural environment and in the pharmaceutical industry.

2. Materials and methods

2.1. Materials

Glucose, sucrose, sorbitol, glycerol, tween 20, CS (Mw of 50-190 kDa, with 75-85% deacetylation ratio), γ-PGA-Na (Mw of 15-50 kDa), EDC, and Sulfo-NHS were purchased from Sigma Chemical Co (St. Louis, MO, USA). Dialysis Tubing with cut-off 12 kD MWCO was purchased from Biotech CE (USA). All other chemicals used in the study were of analytical grade.

2.2. CS-g-PGA synthesis

CS-g-PGA was synthetized as the molar ratio of $[NH_2]/[COOH]$ = 1/ 1. In brief, CS was dissolved in 2% (w/v) acetic acid solution and then adjusted pH value at 5.0. Afterward, γ-PGA, EDC, and sulfo- NHS at a molar ratio of 2:2:3 was dissolved in PBS (10 mM, pH = 6.0), and was added to CS solution under stirring (800 rpm, 30 min, 4 °C and then 24 h at 25 °C). Throughout the reaction, the pH of the mixture was kept in the range of 5.0 up to 6.0. The purified CS-g-PGA copolymer was obtained by dialysis (12 kD MWCO) against deionized water for 72 h. In this case, it was assumed that each PGA had at least one CS binding.

Then, 0.2 mg/mL of the purified CS-g-PGA copolymer was subjected to different treatments including: dH_2O with different pH values, PBS (0.001 M and 0.01 M, pH = 6.0), and dH_2O (pH = 6.0) composed of Glucose (1.0 M), Sucrose (0.5 M), Sorbitol (1.1 M), Glycerol (1.2 M) and Tween 20 (0.06 mM). The amount of additives were selected in the middle of the recommended concentration ranges by Bondos and Bick-nell [**32**].

2.3. Characterization

Frozen samples at a concentration of 0.2 mg/mL were lyophilized using a Freeze Dryer (SCANVAC Coolsafe™, model 110-4, Denmark), condenser temperature — 110 °C, and pressure 0.2 mbar. The freeze-dried samples were stored at 4 °C for further analysis by FT-IR. Furthermore, solutions at appropriate concentrations (based on method) maintained under stirring at 750 rpm for 1 h, were characterized by CD, DLS, and SDS-PAGE.

2.4. FTIR spectroscopy

The FTIR spectra were recorded on a Thermo Nicolet AVATAR 370 FTIR and 64 scans with a variable path length cell and KBr windows. The cell path length was kept constant during all experiments. For each spectrum, a 64-scan interferogram was collected in single-beam mode at 25 °C using 8 cm^{-1} resolution. The sample spectra were recorded at a straight baseline of 400-4000 cm^{-1}.

2.5. Circular dichroism

Far-UV CD (AVIV 215 Circular Dichroism Spectrometer; USA) was used to evaluate the effect of different treatments on the secondary structure of γ-PGA in CS-g-PGA solutions in the range of 190-260 nm at a protein concentration of 0.07 mg/ mL (dilution of 0.2 mg/mL to 0.07 mg/ mL by their specific treatments). CH_3COOH and NaOH were used to adjust the pH, and NaCl and KCl were replaced with Na_2HPO_4 and KH_2PO_4 in PBS construction due to the disruption of γ-PGA signal in the presence of chloride ion. The samples were measured in quartz cuvettes with a path length of 1.0 cm at 25 °C and refractive index of 1.333 in aquase solution with a viscosity of 0.997 g/Cm3 where the percentage of secondary structures was obtained through the mean residue ellipticity ($[\theta]_{mrw,\lambda}$) at wavelength λ (Eq. (**1**)) using the CDNN CD spectra deconvolution software (Version 2.1).

$$[\theta]\mathrm{mrw},\lambda = MRW \times \theta\lambda / 10 \times d \times c \qquad (1)$$

where the mean residue weight (MRW) for the peptide bond is calculated as MRW = M/(N^{-1}), M is the molecular mass of the polypeptide chain (Da), N is the number of amino acids in the chain, N^{-1} is the number of peptide bonds, d is the path length (cm), and c is the concentration (g/ml) [**33**].

2.6. Dynamic light scattering

DLS technique was performed by HORIBA SZ-100 (Japan) for evaluation of particle size and zeta potential of the samples. It is based on the Rayleigh scattering of suspended particles by Brownian motion. The hydrodynamic diameters can be determined by illuminating the sample with a laser source that allows appreciating the particle diffusion velocity. Briefly, 1.5 mL of treated samples at the concentration of 0.2 mg/ mL was placed in a polystyrene half-micro cuvette with a path length of 10 mm and measured at 25 C. The viscosity and refraction index were set equal to those specific to water.

2.7. SDS-PAGE electrophoresis

For evaluating various MW aggregates, SDS-PAGE was performed using 6% resolving gel and 5% stacking gel [**34**]. After centrifugation of the solutions at the concentration of 0.2 mg/mL, 2 μL loading dye was added to 20 iL of the pellet and heated at 95 °C for 5 min. Thereafter, the samples were loaded on 6% SDS-PAGE gel, initially run at 70 V until the dye passed through the stacking gel and then at 110 V. After electrophoretic separation, silver staining was used to detect the different MW of copolymer [**35**].

2.8. Software

All experiments were conducted at least three times, and data were presented as mean ± SD. CDNN2.1 software analysis was utilized to obtain information about the secondary structure of PGA. Statistical analysis was carried out using Excel program version 2010. All figures provided in MS are original and were created by the authors using the BioRender online site and Chemdraw and PowerPoint software.

3. Result and discussions

Whereas, the poly electrostatic interaction of PGA and CS has been studied, their covalent bonding was studied here. As shown in **Fig. 1**, carboxylic acids and amine groups in the lateral branches of PGA and CS, respectively, produce strong electrostatic interactions that are essentially pH-dependent and can be easily self-assembled using physical mixing as a polyelectrolyte structure. In both polymers, some intrinsic structural parameters strongly restrict the behavior of the polymer, such as solubility, stability, size, and surface charge. For example, deacetylation affects the solubility of CS as CS is completely deacetylated due to the protonation of all primary amino groups, showing high solubility in acidic solution [**36**].Park et al. also indicated that if the degree of deacetylation was more than 20%, the formation of a locked crystalline structure is inhibited owing to intra- and/or intermolecular hydrogen bonding within the haphazard distribution of N-acetyl groups of CS [**37**]. Therefore, a copolymer was designed with low molecular polymers and a 75% degree of deacetylation, which can be utilized as a drug delivery system. Also, the grafting between the PGA carboxyl group and the CS amine occurred in the presence of a catalyst (NHS-EDC) at moderate conditions (pH 5-6), so the oxidative agent did not affect the degree of acetylation. It is expected that it has been preserved during the reaction. However, the chemical crosslinking by amide binding increased the physicochemical stability of the resultant co-polymer, but its solubility, stability, and folding were strongly altered by pH, salt and co-solvent concentration.

However, NMR and X-ray crystallography are the only two methods that can be applied to the study of three-dimensional molecular structures of proteins at atomic resolution, NMR spectroscopy is the only method that allows the determination of three-dimensional structures of proteins molecules in the solution phase. NMR spectroscopy can be applied to structure determination by routine NMR techniques for proteins in the size range between 5 and 25 kDa [**38**]. For many proteins in this size range structure determination is relatively easy, however there are many examples of structure determinations of proteins, which have failed due to problems of aggregation and dynamics and reduced solubility. Therefore, due to the high molecular weight of CS-g-PGA that was very higher than the 25 KDa, obtaining suitable NMRs from CS-g-PGA samples at different pH and co-solvents was limited. Especially, because of the accumulation problems and reduced solubility at different pH and co-solvents.

In return, circular dichroism (CD) is an excellent tool for the rapid determination of the secondary structure and folding properties of proteins. While CD does not give the secondary structure of specific residues, as do X-ray crystallographic and NMR structural determinations, the method has the advantage that data can be collected and analyzed in a few hours on solutions of samples containing 20 μg or less of protein in aqueous buffers under physiological conditions [**39**]. Secondary structure can also be estimated from Fourier transform infrared spectroscopy of proteins (FTIR) [**9,40**] and Raman spectroscopy [**41**]. In this study, we studied conformational changes of PGA in different solutions containing co-solvents and different pH values, which could not applicable with NMR. Therefore, we used FTIR, DLS, and SDS-PAGE to confirm these changes.

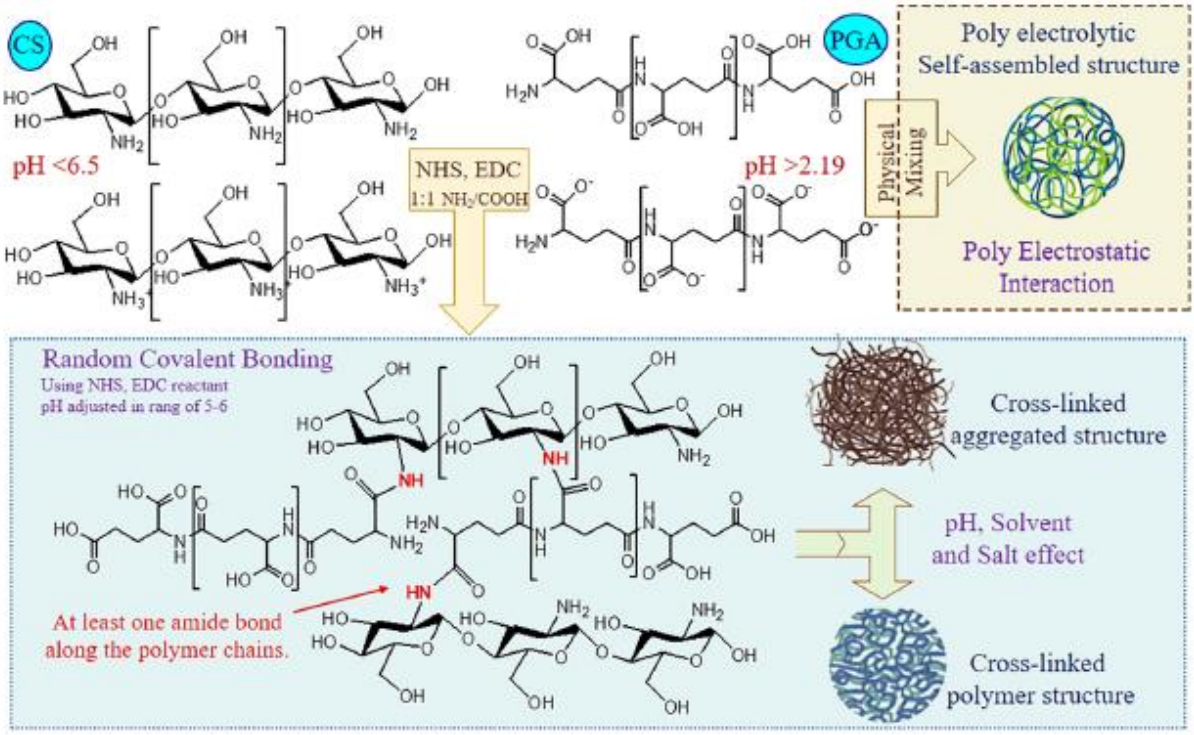

Fig. 1. Chemical structure of CS, PGA under neutral and ionization conditions; Comparison of the polyelectrostatic interaction of PGA and CS from physical mixing with the grafted CS-g-PGA copolymer with at least one covalent bond.

3.1. FTIR analysis of secondary structure of CS-g-PGA

FTIR spectroscopy is an appropriate technique for the study of molecular interactions, secondary structure, and conformation of a wide range of protein solutions. Therefore, grafting of CS onto γ-PGA was confirmed by comparing the infrared spectrum of CS-g-PGA copolymer with the spectra of CS and γ-PGA neat (**Fig. 2**A). The position of characteristic peaks in both the polymer spectrum (CS and γ-PGA) with dash lines were specified in **Fig. 2** (A-D). In the characteristic peaks of γ-PGA, the broad peak at 3450 cm^{-1} corresponded to non-hydrogen-bonded N—H, and the shoulder, which appears at around 3306 cm^{-1}, was attributed to hydrogen-bonded N—H stretching. The carbonyl group of the carboxylic acid (COOH/COO-) was considered as asymmetric and symmetric stretching at about 1580 and 1404 cm^{-1}, respectively. In this area, the peak around 1655 cm^{-1} primarily originated from the C—O stretching vibration in the γ-PGA amide group [**15**]. IR spectra of CS powder also showed two peaks around 930 cm^{-1} and 1068 cm^{-1} corresponding to saccharide structure. The other characteristic peaks were assigned to 3450 (OH and NH_2 stretching), 2889 (—CH stretching), 1659 (amide I), 1597 (amide II), 1381 (C—N stretching), and 1095 cm^{-1} (asymmetric C—O—C stretching). In the CS-g-PGA copolymer, grafting was supported by amide I and amide II bands at 1655 cm^{-1} and 1543 cm^{-1}, which occurred through amidation reaction between branched carboxyl groups in γ-PGA and branched amino groups in CS [**42**]. Comparing IR spectra of γ-PGA and CS with CS-g-PGA represented that the peptide bond in the γ-PGA backbone (C=O and N—H of amide in 1655 and 2950-3600 cm^{-1}) has not changed essentially. While characteristic peaks of the branched carboxylic acid groups at 1580 and 1404 cm^{-1} in proportion to the grafting yield were weakened.

After treatment, the peak of hydrogen-bonded N—H (3306 cm^{-1}) was seen only at pH 3.0, 4.0 (**Fig. 2**B) and in the presence of salt as a shoulder (**Fig. 2**C) and completely disappeared in the presence of cosolvents (**Fig. 2**D). Nonetheless, increasing pH and salt concentration caused decreasing in the

shoulder intensity due to the dissociation of hydrogen bonds. A distinct peak around 1736 cm^{-1} at pH 3.0, which gradually disappeared with increasing pH, could be assigned to the C—O stretching in the COOH branch. With increasing pH and deprotonation of COOH, the asymmetric stretching of COO^- shifted to 1547 cm^{-1}, while no shift was observed in symmetric stretching at 1404 cm^{-1} (**Fig. 2**B). Salt concentration also affect stretching of COO^-, as increasing salt concentration led to the gradual disappearance of asymmetric stretching of COO^-. Interesting, there is no shifting of COO^- asymmetric stretching around 1580 cm^{-1} in the presence of cosolvents.

The results indicate that these treatments affect the intermolecular and intramolecular interactions. So that intramolecular non-hydrogen bonds are the dominant molecular force associated with CS-g-PGA, and the small shift of COO^- asymmetric stretching in different concentration of salt and pH values can also arise from electrostatic interaction between the amino groups of CS and carboxyl group of γ-PGA, which is neutralized in the presence of different co-solvents. Generally, the most probable intermolecular interactions in γ-PGA molecules are electrostatic repulsion and chain entanglement. Nonetheless, in the presence of CS, protonated amino groups (μI 6.5) interact electrostatically with the deprotonated carboxylate of γ-PGA (μI 2.19) at lower pH values. The intermolecular electrostatic interactions are disappeared in the presence of a high concentration of salt and co-solvents owing to their effect on the dielectric constant of the solution and the strength of hydrophobic interactions [**31**].

The effect of various treatments on γ-PGA structure in CS-g-PGA was also examined by FTIR to distinguish the conformational transitions. In this regard, protein solubility would enhance the α-helix structure [**43**] and accompany a sharp change of solubility by switching between assembly and disassembly, which is triggered by the structural α-helix or β-sheet to-random transitions [**44**]. The infrared spectra of amide I and II stretches are related to α-helical structure, while the shifting of the amide I band leads to β-sheet structures, and the amide II band leads to random coils [**8**]. The amide I band at 1655 cm^{-1}, which exhibited α-helical structure, did not change at pH values of 3.0 to 7.0 in comparison to γ-PGA and CS (**Fig. 2**B). The amide II band shifted from 1597 cm^{-1} (CS) to 1580 cm^{-1} (γ-PGA), 1547 cm^{-1} (pH 3.0), and around 1562 cm^{-1} at the other pH values, which confirmed the existence of random coil structure. The band-shifting can be related to the vibrations of $-NH_2$ deformation and the asymmetric stretch of the carboxylate group ($-COO^-$). At low pH, the protonated copolymer will exhibit a helical conformation presumably due to hydrogen bonding. At pH 5.0 to neutral, the unstable negatively charged carboxylate groups will interact with positively to neutral charged CS, which leads to more ordered structures.

The γ-PGA at an ionic strength of 0.001 M exhibited only shifting of the band at 1547 cm^{-1} adapted a random coil conformation in the CS-g-PGA structure (**Fig. 2**C). When the ionic strength was increased to 0.01 M, the structure changed to β-sheet due to the shifting of the band from 1655 cm^{-1} to 1670 cm^{-1}. The data is in accordance with He et al., who confirmed that γ-PGA had a helical conformation at a low ionic strength of the solution and could be changed to a mixture of helix and β-sheet and then predominantly β-sheet with the continuous increase of the ionic strength [**8**]. Salts can affect electrostatic interactions in the copolymer by interacting the anionic and cationic components with the accessible charged or polarized sites and subsequently influencing the conformation of copolymers.

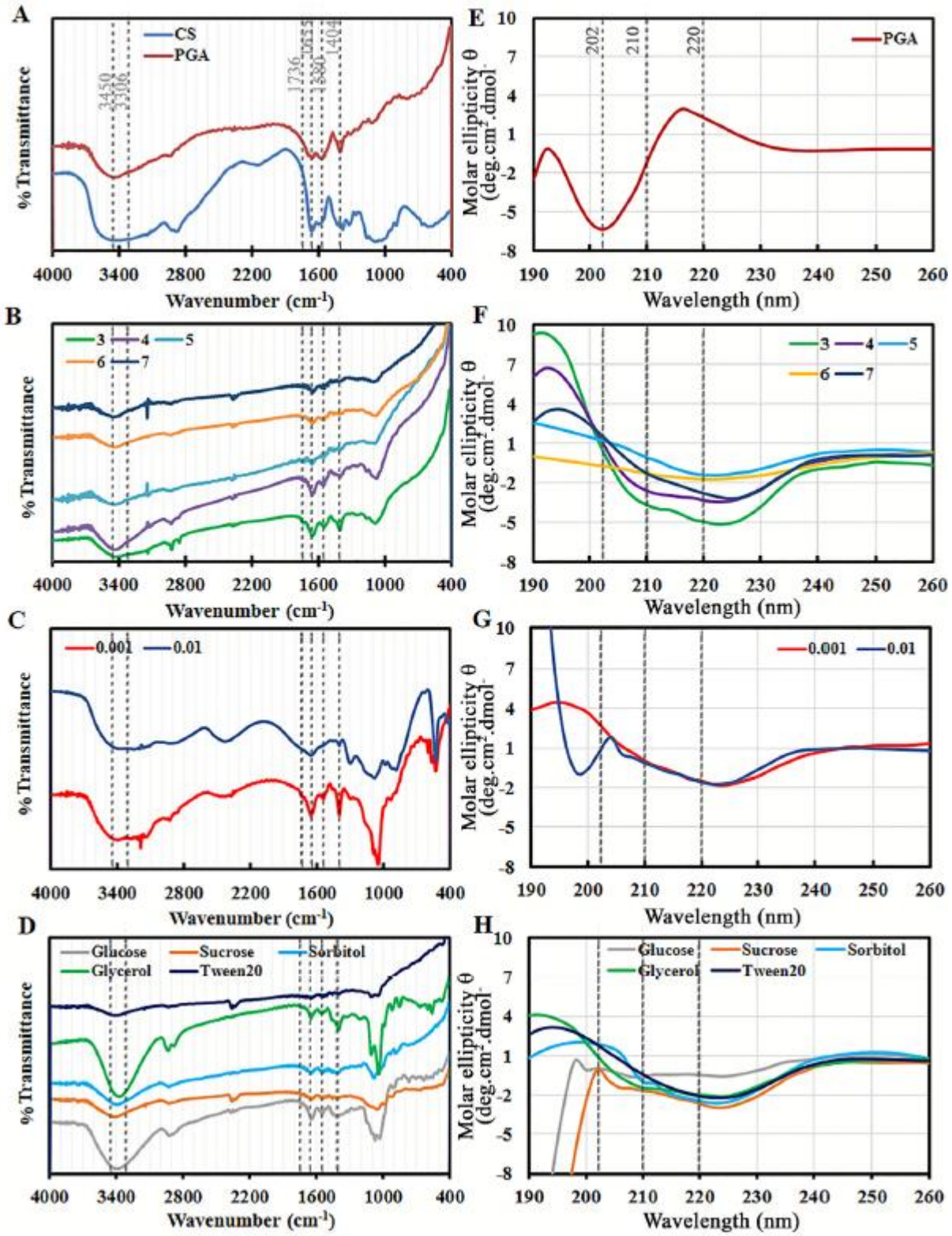

Fig. 2. FT-IR spectra of (A) PGA and CS in respect to CS-g-PGA at (B) pH values of 3-7, (C) Salt concentration of 0.01 and 0.001 M, and (D) Co-solvents (Glucose, Sucrose, Sorbitol, Glycerol and Tween 20); CD spectra of (E) γ-PGA in CS-g-PGA at (F) pH values of 3-7, (G) Salt concentration of 0.01 and 0.001 M, and (H) Cosolvents (Glucose, Sucrose, Sorbitol, Glycerol and Tween 20) were recorded at RT.

In the presence of co-solvents, the amide I band at 1655 cm^{-1}, which exhibited α-helical structure, did not change and preserved the α-helical structure. Nonetheless, the amide II band shifted to 1562 cm^{-1} (Glycerol) and around 1558 cm^{-1} in the presence of other co-solvents, which confirmed the existence of a random coil structure. These alterations can be due to lowering the dielectric constant of the solutions and the strength of hydrophobic interactions by the co-solvents [**31**].

3.2. Secondary structure analysis of γ-PGA by CD spectroscopy

Far-UV CD spectroscopy was used to gain insight into the structural biology and characteristics of γ-PGA in the copolymer (CS-g-PGA). The most common conformation for the ionized and unionized form of γ-PGA will be a random coil and helical, respectively, which characterized as a negative peak after and before 210 nm in CD spectrum, respectively [**14,15**]. The helical conformation is related to the intramolecular hydrogen bonds, but the random coil structure may be attributed to non-hydrogen interactions due to the presence of negatively charged carboxylate groups, the strong electrostatic repulsion, and the lack of the hydrogen bonds [**15**]. As shown in **Fig. 2**E, γ-PGA had a large negative peak at 202 nm and a large positive peak centered at 216 nm, which characterized as an ionized polymer with unordered structure, because γ-PGA-Na was stabilized by hydrogen bonds of its carbonyl groups with solvent instead of intramolecular hydrogen-bonds [**45**]. Nonetheless, the covalent linkage to CS was the first factor that caused dramatic changes in the secondary structure of native γ-PGA. It can be attributed to the presence of amino groups of CS, which minimizes the repulsive interactions among negative side chains of γ-PGA and form ordered structures [**46**]. Therefore, CS can stabilize the secondary structure of γ-PGA by a higher extent of intermolecular and intramolecular interactions in optimized conditions.

Environmental conditions (e.g., pH, and co-solvents) also affect the intramolecular and intermolecular interactions of γ-PGA. To investigate the optimized conditions at which CS-g-PGA will show a more stable structure, CS-g-PGA was analyzed using CD measurements at different treatments. As shown in **Fig. 2**F, by changes in pH of the solution, the spectrum of γ-PGA lost the random coil structure and significantly changed to ordered structures. There were two minima at pH 3.0 and 4.0, 224 nm and 210 nm, which were characteristic of α-helical structures, and pH 3.0 showed the stronger α-helical structure. The represented results in **Fig. 2**F also confirmed that pH 3.0 and 4.0 significantly induced an ordered structure of a-helical and reduced aggregation. Gradually, by increasing pH up to 7.0, the CD spectrum at 210 nm was replaced by a strong minimum at 224 nm, indicating that the secondary structure was going to β-sheet structure. Quite a different profile was observed at pH 5.0, and 6.0 broadening of these spectra at 220-225 nm arose from the contribution of β-sheet, which exhibited redshift (from 215 to 218 to 220-225 nm), that can be attributed to absorption flattening and differential scattering phenomena in the CD spectra of the samples [**47,48**]. Therefore, increasing pH produced a transition from a-helical to primarily p-sheet-rich structure. In detail, **Table 1**, CS-g-PGA at pH 3.0 consisted of the highest α-helix (14.89%) and the lowest antiparallel (40.70%) and parallel (7.86%) sheets, whereas γ-PGA showed the lowest a-helix (9.05%) and the highest antiparallel (48.71%), and parallel (6.92%) at pH 5.0. Higher β-sheet content and lower unordered structures at pH 5.0 suggested that this pH was a reason for self-assembly and aggregate formation [**49**]. pH 6.0 also showed the closest percentages of p-turn (13.17%) and random coil (24.01%) to the y-PGA. According to Mahler et al., treatment of proteins at acidic pH results in cleavage and aggregation, whereas at neutral to alkaline pH caused deamidation and oxidation [**23**]. Such alterations in γ-PGA conformation can be dependent on the electrostatic behavior of functional groups and peptide bonds in the skeleton of the polymer. The rigid planar amidic bond is neither acidic nor basic at physiological pH owing to a partial double bond character, which results from resonance and inhibits free rotation. Nonetheless,

changes in the environmental pH lead to protonation or deprotonation of the groups in addition to the side chains. Therefore, the electronic environment in that region changes drastically, which may influence the protein structure by conformational changes to minimize repulsive interactions and produce new attractive interactions.

Subsequently, CS-g-PGA was treated by a salt concentration of 0.01 and 0.001 M and monitored with CD spectroscopy (**Fig. 2**G). In the presence of salt, CD spectra were also dominated by β-sheets where the α-helix minimum at 210 nm was completely replaced by a minimum at 224 nm. β-sheets are crucial for peptide self-assembly and aggregate formation due to complementary electrostatic interactions and hydrogen bonds [**49**]. CS-g-PGA in salt concentration of 0.01 M also showed a sharp minimum and maximum at 198 nm and 204 nm, which were effectively blue-shifted around 4-12 nm with respect to γ-PGA and indicated more unordered structural component. **Table 1** and **Fig. 2**G also confirmed that PBS significantly affected the native structure of γ-PGA due to the high amount of antiparallel structure and a-helical characters. Salts can affect the protein structure depending on the type (kosmotropic or chaotropic) and concentration. Phosphate anions of PBS as a strong kosmotropic agent will result in a salting-out effect and effectively strengthening the intermolecular interactions in CS-g-PGA molecules. In other words, removing water from the CS-g-PGA shell by salt ions produces thermodynamically unfavorable interactions, which increases with increasing salt concentration generally near pI [**50,51**].

Table 1 Estimated structure fractions, Z-average Size, polydispersity index, and ζ-potential of CS-g-PGA after different treatments.

ζ-potential (mV)	–	−8.10 ± 2.30	11.50 ± 0.20	12.60 ± 0.20	12.80 ± 0.40	13.10 ± 0.30	No detectable	No detectable	No detectable	No detectable	No detectable	No detectable	No detectable
PDI	–	0.60 ± 0.00	0.60 ± 0.10	3.70 ± 0.30	0.70 ± 0.10	1.50 ± 0.90	1.40 ± 0.40	2.30 ± 1.40	1.20 ± 1.10	1.20 ± 0.40	0.70 ± 0.30	1.00 ± 0.60	2.20 ± 0.60
Z-average (μm)	–	1.10 ± 0.10	0.90 ± 0.20	4.00 ± 3.00	1.60 ± 0.40	3.60 ± 0.60	5.20 ± 2.40	3.80 ± 1.20	2.90 ± 2.20	2.40 ± 0.90	2.10 ± 1.50	2.20 ± 1.00	3.70 ± 2.60
Random coil	28.46	23.60	23.00	23.00	24.00	23.70	22.30	22.80	23.70	28.10	22.90	22.80	23.20
β-Turn	20.50	12.80	12.60	12.30	13.20	12.40	11.90	12.30	13.10	14.50	12.40	12.60	12.40
Parallel	4.59	7.90	7.50	6.90	6.70	7.20	7.30	7.10	6.40	5.70	7.50	7.20	7.10
Anti parallel	39.79	40.70	44.28	48.71	46.93	45.72	48.10	48.14	49.11	44.30	45.48	47.01	47.14
Helix	6.65	14.90	12.40	9.00	9.10	10.80	10.20	9.60	7.60	7.30	11.70	10.40	10.10
Treatment	–	3.0	4.0	5.0	6.0	7.0	0.001	0.010	Glucose	Sucrose	Sorbitol	Glycerol	Tween 20
	Native State	pH					Salt concentration (M)		Co-Solvent				
Sample	γ-PGA	CS-g-PGA											

We also investigated the effects of co-solvents on the secondary structure of CS-g-PGA (**Fig. 2**H). Interestingly, it showed the further flattening at 224 nm, a definite p-sheet transition, which is likely due to differential absorption flattening. Nonetheless, there was a mess at 195-210 nm, as a peak of 210 nm for sorbitol contributed to α-helical structure, and blue-shifted peaks of maxima around 198 and 202 nm with decreased magnitude and the effective disappearance of minima in the presence of glucose and sucrose related to random coil structure. **Fig. 2**H and **Table 1**, also showed little changes in α-helix (7.35%), antiparallel (44.30%), parallel (5.69%), β-turn (14.52%), and random coil (28.12%) in the presence of sucrose. These results suggested that sucrose might be an effective preservative for the native structure of γ-PGA in CS-g-PGA. This data is in accordance with Prestrelski et al., who confirmed the inhibition of random coil to β-sheet transition in poly-L-lysine by sucrose, but mono-saccharide such as glucose was ineffective as a stabilizer [**29**]. The other co-solvents effectively interfered with the intermolecular and intramolecular interactions, and the highest percentage of α-helix (11.71%) and antiparallel (49.11%) belonged to sorbitol and glucose, respectively (**Fig. 2**H and **Table 1**). Therefore the increase of α-helix and β-sheet and decrease of random coil and β-turn in the

γ-PGA structure of CS-g-PGA were considered to be the main responsible for the conformational variation at different treatments.

3.3. Evaluation of $\mathbb{Z}$-average size, polydispersity index (PDI), and zeta potential

Herein, DLS was utilized for comparing the amount of CS-g-PGA aggregation qualitatively by evaluation of $\mathbb{Z}$-average size, PDI and Zeta potential. Different studies determined the sizes of fresh proteins using DLS at constant temperature to confirm the conformational properties of proteins. Wang et al., used DLS to compare size of PGA at various pH values [**15**]. Hauptmann et al., used DLS to measure the size and distribution of nanometer and submicron monoclonal antibodies [**52**]. However, Borzova et al., studied the kinetics of thermal aggregation of BSA using DLS [**4**]. Herein, size and polydispersity index of product with and without additives were done in fresh samples. Due to the unstable thermodynamic nature of the copolymer under aggregation conditions, the size of the aggregated structure changes over the time of analysis and increases the uncertainty of z-average size and PDI [**53,54**]. Therefore the standard deviation (SD) in size and PDI, determined by DLS in iterative measurements, can be used as a criterion for confirming structure instability and aggregation production. In contrast, the decrease in the zeta potential of the copolymer nanostructure (less than ±10 mV) is associated with increased thermodynamic instability due to hydrophobicity. Therefore, it is expected that the aggregated structure in DLS and zeta analysis will be confirmed with the large z-average size, high PDI (> 0.6) and low zeta potential (|±10mV| >). As reported in **Table 1** (**Fig. 1**S-A), comparison of plots after pH treatments showed the smallest particle size and PDI at pH values of 3.0 (1.07 ± 0.07 |μm, 0.61 ± 0.04) and 4.0 (0.92 ± 0.22 im, 0.58 ± 0.09) and then the appearance of a significant increment Z-average size (4.05 ± 3.00) and PDI (3.72 ± 3.27) at pH 5.0. Thereafter, the size of the copolymer decreased to 1.58 ± 0.40 im as pH increased to 6.0 and upon increasing the pH to 7.0, the size was accompanied by a dramatic increase (3.63 ± 0.57) in scattered intensity (1.48 ± 0.86). According to the PDI values of highly polydisperse (~0.1) and monodisperse (<0.6) samples [**5**], the alteration of the pH can induce, inhibit, or potentiate the copolymer aggregation. These changes can be related to their pI values of both components, as each component have a tendency of either attracting protons at a pH below their pI or giving up protons at a pH above their pI, which leads to positive to negative charges on y-PGA and positively charged to neutral on CS. Therefore, while because of γ-PGA carboxylic groups its charge is negative in pure conditions, at low pH values, the positive charge of amine groups of CS is predominant and the net charge of CS-g-PGA was positive and induced repulsive forces and then a low tendency to accumulate. By increasing the pH up to 7.0, slow deprotonation of CS and y-PGA reduces the positive charge of CS and vice versa increases the negative charge of γ-PGA. The exact balance between hydrogen bond formation, electrostatic interaction and hydrophobicity increases sediment formation, while solubility increased due to the fragile equilibrium in the narrow pH range close to pH 6.0, which are consistent with FTIR data. As expected, the zeta potential at different pHs was negligible by confirming the evidence of the z-average size. This condition is exacerbated by increasing the salt concentration and adding co-solvent, so that the zeta potential shifts to smaller values (< 10 mV) which due to its large uncertainty is reported as “no detectable” in **Table 1**.

Comparing the Z-average size and PDI for 0.01 M (3.81 ± 1.18 im and 2.28 ± 1.41) and 0.001 M (5.25 ± 2.39 μm and 1.36 ± 0.36) demonstrated that increasing salt concentration induced aggregation (**Table 1**; **Fig. 1**S-B). At low ionic strength, the salt can stabilize γ-PGA through the attraction of oppositely counter ions at the copolymer surface. At high ionic strength, however, salts exert specific effects on proteins depending on the type and concentration, resulting in either the stabilization or destabilization of proteins or even denaturation [**10**]. In this study, PBS caused the entanglement of the constructor and increased Z-Average and PDI values. However, the effects of salts on protein

stability are closely correlated with the salting-out effect which increases the stability of proteins [**10,11**].

Finally, DLS measurements also indicated heterodispersity and aggregation in the presence of co-solvents in constant copolymer concentration (**Table 1**, **Fig. 1**S-C). It was expected that these small and molecularly flexible co-solvents grouped into uncharged sugars (glucose and sucrose) and polyols (sorbitol and glycerol) produced a monodisperse particle distribution in the solution due to the miscibility, formation of hydrogen bonds, less sterically hindered in interacting and tighter packing [**55**]. By contrast, the solution containing glucose exhibited an increase of 2.91 ± 2.25 im to sorbitol 2.08 ± 1.55 im, which rationalized by alterations in reaction kinetics and thermodynamic considerations. In this case, the co-solvents were excluded from the protein surface and resulted in molecular mobility of the protein in an unfolding and most other modes of degradation. Thereafter, water formed hydrogen bonding with the protein, and the copolymer was increasingly hydrated. These molecular mobility and protein hydration both resulted in aggregation and a possible reason for the increase of Z-average size and PDI [**11,52,55**]. In other words, uncharged sugars and polyols seem to exclude preferentially from the protein-water interface and destabilize the CS-g-PGA. According to Ohtake et al., a surfactant such as Tween 20 should exhibit a greater protective effect than uncharged sugars [**11**]. Interestingly, in the case of CS-g-PGA, the presence of Tween 20 did not prevent the aggregate formation and showed a remarkable increase of the mean hydrodynamic radius (3.74 ± 2.62 im) and polydispersity (2.21 ± 2.60). Nonetheless, the mechanism of Tween 20 binding and stabilizing/destabilizing of the protein is not clear yet. However, it has to be mentioned that the action of co-solvents is extremely pH [**1**] and concentration [**9**] dependent, and this analysis should be continued at different concentrations and pH values.

3.4. Evaluation of CS-g-PGA fragments by SDS-PAGE electrophoresis

SDS-PAGE cannot confirm conformational changes of the copolymer, but it is considered a valuable tool to analyze small-size aggregates and differentiate their various MW. SDS as an anionic detergent denatures proteins and gives the copolymer a negative charge. Then during the heating at high temperature, the existing protein aggregates may be fully dissolved [**23**]. The covalent linkage of γ-PGA to CS can dramatically alter the γ-PGA structure and the aggregation properties. Even though the different treatments were assayed to search for conditions that will prevent or minimize aggregation.

As shown in supplementary data **Fig. 1**S (D—F), the intensities of the stained bands demonstrated the heterogeneous Mw of the CS-g-PGA after different treatments. At different pH values, the major fragments of the copolymer were separated at 15—40 kDa, 70 kDa, and very low-intensity bands between 100 and 130 kDa. While the high-intensity bands ranging in size from 15 to 170 kDa exhibited at a salt concentration of 0.01 and 0.001. As expected, in the presence of additives, the copolymer primarily indicated the bands below 130 kDa. Due to the sedimentary nature of the sample in the aggregated structures, smire bands in SDS induced a darker appearance in GEL. These results confirmed that different treatments influenced the aggregation behavior of the copolymer, and pH was the most effective factor to reduce the aggregation, but salt concentration could increase the varieties of the fragments and the amount of aggregation. These results confirmed that SDS-PAGE assay in accompany with DLS analysis are generally applicable for evaluating the aggregation behavior of CS-g-PGA.

4. Conclusion

This study was aimed at understanding the effect of CS, co-solvents, different pH values, and salt concentration on the decrease of attractive protein interactions, suppression, and dissolution of aggregations. The comparable analysis revealed the different results encompassed: (i) Grafting of CS to γ-PGA was the first parameter to affect the conformational structure of γ-PGA, (ii) the aggregation proceeded in the presence of sugars, polyols, and surfactant at the specified concentration and pH, (iii) Lower concentration of PBS was more effective than higher concentration in reducing visible protein aggregation, and (iv) Owing to the polyelectrolyte characteristics of the polymers, pH plays a key role in stabilizing γ-PGA with the smallest aggregation and conformational change. They can influence the orientation of side chains, the apparent charge, and consequently, the overall conformation and local structure of the biopolymer. Therefore, the concentration and pH value of the cosolvents have to be considered for the suppression or induction of aggregation in future work.

References

[1] L. Galm, J. Morgenstern, J. Hubbuch, Manipulation of lysozyme phase behavior by additives as function of conformational stability, Int. J. Pharm. 494 (2015) 370—380.

[2] L. Nielsen, S. Frokjaer, J.F. Carpenter, J. Brange, Studies of the structure of insulin fibrils by Fourier transform infrared (FTIR) spectroscopy and electron microscopy, J. Pharm. Sci. 90 (2001) 29—37.

[3] S.K. Chaturvedi, M.K. Siddiqi, P. Alam, R.H. Khan, Protein misfolding and aggregation: mechanism, factors and detection, Process Biochem. 51 (2016) 1183—1192.

[4] V.A. Borzova, K.A. Markossian, N.A. Chebotareva, S.Y. Kleymenov, N.B. Poliansky, K.O. Muranov, V.A. Stein-Margolina, V.V. Shubin, D.I. Markov, B.I. Kurganov, Kinetics of thermal denaturation and aggregation of bovine serum albumin, PLoS One 11 (2016), e0153495.

[5] J. Dobson, A. Kumar, L.F. Willis, R. Tuma, D.R. Higazi, R. Turner, D.C. Lowe, A. E. Ashcroft, S.E. Radford, N. Kapur, Inducing protein aggregation by extensional flow, Proc. Natl. Acad. Sci. 114 (18) (2017) 4673—4678.

[6] R. Liu, R. Su, M. Liang, R. Huang, M. Wang, W. Qi, Z. He, Physicochemical strategies for inhibition of amyloid fibril formation: an overview of recent advances, Curr. Med. Chem. 19 (2012) 4157—4174.

[7] R. Mehra, B. Dehury, K.P. Kepp, Cryo-temperature effects on membrane protein structure and dynamics, Phys. Chem. Chem. Phys. 22 (2020) 5427—5438.

[8] L. He, M. Neu, L. Vanderberg, Bacillus lichenformis y-glutamyl exopolymer: physicochemical characterization and U (VI) interaction, Environ. Sci. Technol. 34 (2000) 1694—1701.

[9] K.C. Bauer, S. Suhm, A.K. Wáll, J. Hubbuch, Impact of additives on the formation of protein aggregates and viscosity in concentrated protein solutions, Int. J. Pharm. 516 (2017) 82—90.

[10] H. Hamada, T. Arakawa, K. Shiraki, Effect of additives on protein aggregation, Curr. Pharm. Biotechnol. 10 (2009) 400—407.

[11] S. Ohtake, Y. Kita, T. Arakawa, Interactions of formulation excipients with proteins in solution and in the dried state, Adv. Drug Deliv. Rev. 63 (2011) 1053—1073.

[12] I. Khalil, A. Burns, I. Radecka, M. Kowalczuk, T. Khalaf, G. Adamus, B. Johnston, M. Khechara, Bacterial-derived polymer poly-γ-glutamic acid (γ-PGA)-based micro/nanoparticles as a delivery system for antimicrobials and other biomedical applications, Int. J. Mol. Sci. 18 (2017) 313.

[13] R. Ahmad, Y. Deng, R. Singh, M. Hussain, M.A.A. Shah, S. Elingarami, N. He, Y. Sun, Cutting edge protein and carbohydrate-based materials for anticancer drug delivery, J. Biomed. Nanotechnol. 14 (2018) 20—43.

[14] I. Hajdu, M. Bodnar, G. Filipcsei, J.F. Hartmann, L. Daroczi, M. Zrínyi, J. Borbely, Nanoparticles prepared by self-assembly of chitosan and poly-γ-glutamic acid, Colloid Polym. Sci. 286 (2008) 343—350.

[15] L.-L. Wang, J.-T. Chen, L.-F. Wang, S. Wu, G.-z. Zhang, H.-Q. Yu, X.-d. Ye, Q.-S. Shi, Conformations and molecular interactions of poly-γ-glutamic acid as a soluble microbial product in aqueous solutions, Sci. Rep. 7 (2017) 12787.

[16] I.R. Khalil, A.T. Burns, I. Radecka, M. Kowalczuk, T. Khalaf, G. Adamus, B. Johnston, M.P. Khechara, Bacterial-derived polymer poly-γ-glutamic acid (γ-PGA)-based micro/nanoparticles as a delivery system for antimicrobials and other biomedical applications, Int. J. Mol. Sci. 18 (2017) 313.

[17] S.A. Papadimitriou, D.S. Achilias, D.N. Bikiaris, Chitosan-g-PEG nanoparticles ionically crosslinked with poly (glutamic acid) and tripolyphosphate as protein delivery systems, Int. J. Pharm. 430 (2012) 318—327.

[18] M. Motiei, S. Kashanian, L.A. Lucia, M. Khazaei, Intrinsic parameters for the synthesis and tuned properties of amphiphilic chitosan drug delivery nanocarriers, J. Control. Release 260 (2017) 213—225.

[19] D.-Y. Ji, T.-F. Kuo, H.-D. Wu, J.-C. Yang, S.-Y. Lee, A novel injectable chitosan/ polyglutamate polyelectrolyte complex hydrogel with hydroxyapatite for soft-tissue augmentation, Carbohydr. Polym. 89 (2012) 1123—1130.

[20] H.-D. Wu, J.-C. Yang, T. Tsai, D.-Y. Ji, W.-J. Chang, C.-C. Chen, S.-Y. Lee, Development of a chitosan—polyglutamate based injectable polyelectrolyte complex scaffold, Carbohydr. Polym. 85 (2011) 318—324.

[21] A. Nieto-Orellana, H. Li, R. Rosiere, N. Wauthoz, H. Williams, C.J. Monteiro, C. Bosquillon, N. Childerhouse, G. Keegan, D. Coghlan, Targeted PEG-poly (glutamic acid) complexes for inhalation protein delivery to the lung, J. Control. Release 316 (2019) 250—262.

[22] J. Jacobs, G. Pound-Lana, B. Klumperman, Poly (N-vinylpyrrolidone-b-(γ-benzyl-l-glutamate))—synthesis and self-assembly into pH-sensitive micelles, Polym. Chem. 3 (2012) 2551—2560.

[23] H.C. Mahler, W. Friess, U. Grauschopf, S. Kiese, Protein aggregation: pathways, induction factors and analysis, J. Pharm. Sci. 98 (2009) 2909—2934.

[24] A. Di Martino, P. Kucharczyk, J. Zednik, V. Sedlarik, Chitosan grafted low molecular weight polylactic acid for protein encapsulation and burst effect reduction, Int. J. Pharm. 496 (2015) 912—921.

[25] A.M. de Oliveira, E. Jáger, A. Jáger, P. Stepanek, F.C. Giacomelli, Physicochemical aspects behind the size of biodegradable polymeric nanoparticles: a step forward, Colloids Surf. A Physicochem. Eng. Asp. 436 (2013) 1092—1102.

[26] Y.H. Kim, S.H. Gihm, C.R. Park, K.Y. Lee, T.W. Kim, I.C. Kwon, H. Chung, S. Y. Jeong, Structural characteristics of size-controlled self-aggregates of deoxycholic acid-modified chitosan and their application as a DNA delivery carrier, Bioconjug. Chem. 12 (2001) 932—938.

[27] P.M. Moreno, J.C.D.C. Santos, C.P. Gomes, A. Varela-Moreira, A. Costa, V. Leiro, H. S. Mansur, A.P. Pego, Delivery of splice switching oligonucleotides by amphiphilic chitosan-based nanoparticles, Mol. Pharm. 13 (2) (2015) 344—356.

[28] S. Anwar, R.K. Kar, M.A. Haque, R. Dahiya, P. Gupta, A. Islam, F. Ahmad, M. I. Hassan, Effect of pH on the structure and function of pyruvate dehydrogenase kinase 3: combined spectroscopic and MD simulation studies, Int. J. Biol. Macromol. 147 (2020) 768—777.

[29] S.J. Prestrelski, N. Tedeschi, T. Arakawa, J.F. Carpenter, Dehydration-induced conformational transitions in proteins and their inhibition by stabilizers, Biophys. J. 65 (1993) 661—671.

[30] S.N. Timasheff, Protein-solvent preferential interactions, protein hydration, and the modulation of biochemical reactions by solvent components, Proc. Natl. Acad. Sci. 99 (2002) 9721—9726.

[31] R.M. Kramer, V.R. Shende, N. Motl, C.N. Pace, J.M. Scholtz, Toward a molecular understanding of protein solubility: increased negative surface charge correlates with increased solubility, Biophys. J. 102 (2012) 1907-1915.

[32] S.E. Bondos, A. Bicknell, Detection and prevention of protein aggregation before, during, and after purification, Anal. Biochem. 316 (2003) 223-231.

[33] S.M. Kelly, T.J. Jess, N.C. Price, How to study proteins by circular dichroism, Biochim. Biophys. Acta (BBA)-Protein Proteome. 1751 (2005) 119-139.

[34] J. Sambrook, D.W. Russell, SDS-polyacrylamide gel electrophoresis of proteins, CSH Protoc. 1 (2006) 4.

[35] M. Chevallet, S. Luche, T. Rabilloud, Silver staining of proteins in polyacrylamide gels, Nat. Protoc. 1 (2006) 1852.

[36] I.A. Sogias, V.V. Khutoryanskiy, A.C. Williams, Exploring the factors affecting the solubility of chitosan in water, Macromol. Chem. Phys. 211 (2010) 426-433.

[37] J.H. Park, Y.W. Cho, H. Chung, I.C. Kwon, S.Y. Jeong, Synthesis and characterization of sugar-bearing chitosan derivatives: aqueous solubility and biodegradability, Biomacromolecules 4 (2003) 1087-1091.

[38] F.M. Poulsen, A Brief Introduction to NMR Spectroscopy of Proteins, 2002.

[39] N.J. Greenfield, Using circular dichroism spectra to estimate protein secondary structure, Nat. Protoc. 1 (2006) 2876.

[40] M. Jackson, H.H. Mantsch, The use and misuse of FTIR spectroscopy in the determination of protein structure, Crit. Rev. Biochem. Mol. Biol. 30 (1995) 95-120.

[41] J.T. Pelton, L.R. McLean, Spectroscopic methods for analysis of protein secondary structure, Anal. Biochem. 277 (2000) 167-176.

[42] J. Xu, D. Solaiman, R.D. Ashby, R.A. Garcia, S.H. Gordon, R.E. Harry-O'kuru, Properties of starch-polyglutamic acid (PGA) graft copolymer prepared by microwave irradiation— Fourier transform infrared spectroscopy (FTIR) and rheology studies, Starch-Stárke 69 (2017) 1600021.

[43] D. Matsui, S. Nakano, M. Dadashipour, Y. Asano, Rational identification of aggregation hotspots based on secondary structure and amino acid hydrophobicity, Sci. Rep. 7 (2017) 9558.

[44] T. Waku, N. Hirata, M. Nozaki, K. Nogami, S. Kunugi, N. Tanaka, Morphological transformation of peptide nanoassemblies through conformational transition of core-forming peptides, Polymers 11 (2019) 39.

[45] J.L. Lopes, A.J. Miles, L. Whitmore, B.A. Wallace, Distinct circular dichroism spectroscopic signatures of polyproline II and unordered secondary structures: applications in secondary structure analyses, Protein Sci. 23 (2014) 1765-1772.

[46] M. Colaco, J. Park, H. Blanch, The kinetics of aggregation of poly-glutamic acid based polypeptides, Biophys. Chem. 136 (2008) 74-86.

[47] C.S. Starck, A.J. Sutherland-Smith, Cytotoxic aggregation and amyloid formation by the myostatin precursor protein, PLoS One 5 (2010), e9170.

[48] N. Bijari, S. Balalaie, V. Akbari, F. Golmohammadi, S. Moradi, H. Adibi, R. Khodarahmi, Effective suppression of the modified PHF6 peptide/1N4R tau amyloid aggregation by intact curcumin, not its degradation products: another evidence for the pigment as preventive/therapeutic "functional food", Int. J. Biol. Macromol. 120 (2018) 1009-1022.

[49] Y. Liu, L. Zhang, W. Wei, Effect of noncovalent interaction on the self-assembly of a designed peptide and its potential use as a carrier for controlled bFGF release, Int. J. Nanomedicine 12 (2017) 659.

[50] L. Zongo, H. Lange, C. Crestini, A study of the effect of Kosmotropic and Chaotropic ions on the release characteristics of lignin microcapsules under stimuli-responsive conditions, ACS Omega 4 (2019) 6979-6993.

[51] L. Zhang, H. Tan, R.M. Fesinmeyer, C. Li, D. Catrone, D. Le, R.L. Remmele Jr., J. Zhang, Antibody solubility behavior in monovalent salt solutions reveals specific anion effects at low ionic strength, J. Pharm. Sci. 101 (2012) 965-977.

[52] A. Hauptmann, K. Podgorsek, D. Kuzman, S. Srcic, G. Hoelzl, T. Loerting, Impact of buffer, protein concentration and sucrose addition on the aggregation and particle formation during freezing and thawing, Pharm. Res. 35 (2018) 101.

[53] K.L. Zapadka, F.J. Becher, A. Gomes dos Santos, S.E. Jackson, Factors affecting the physical stability (aggregation) of peptide therapeutics, Interface Focus 7 (2017) 20170030.

[54] G. Singh, I. Brovchenko, A. Oleinikova, R. Winter, Peptide aggregation in finite systems, Biophys. J. 95 (2008) 3208-3221.

[55] M.A. Mensink, H.W. Frijlink, K. van der Voort Maarschalk, W.L. Hinrichs, How sugars protect proteins in the solid state and during drying (review): mechanisms of stabilization in relation to stress conditions, Eur. J. Pharm. Biopharm. 114 (2017) 288-295.